Comparative Biochemistry and Physiology, Part B 253 (2021) 110547

Contents lists available at ScienceDirect

Comparative Biochemistry and Physiology, Part B

journal homepage: www.elsevier.com/locate/cbpb

Change on apoptosis, autophagy and mitochondria of the Harderian gland in *Cricetulus barabensis* during age

Xiao-Tong Kong [1,2], Zhe Wang [1,2], Jun-Jie Mou [1,2], Chang-Sheng Li, Hui-Liang Xue, Ming Wu, Lei Chen, Jin-Hui Xu [*], Lai-Xiang Xu

College of Life Sciences, Qufu Normal University, 273165 Qufu, Shandong, China

ARTICLE INFO

Keywords:
Striped dwarf hamsters
Cricetulus barabensis
Autophagy
Apoptosis
Harderian gland
Aging
Mitochondrion fission

ABSTRACT

Harderian gland (HG) plays an important role in the physiological adaptation to terrestrial life, however, the mechanisms underlying the changes in the structure and function of the HG during aging remain unclear. This study investigated autophagy and apoptosis in the HG of striped dwarf hamsters (*Cricetulus barabensis*) of different ages (sub-adult, adult and aged groups) in both males and females. The results showed that LC3II/LC3I and puncta of LC3 were significantly higher in adult and aged individuals than sub-adults, whereas P62 decreased with age. Bax/bcl2was the highest in sub-adults of male and female individuals. Caspase3 activity was the highest in sub-adults of male and female individuals, and the citrate synthase activity was highest in sub-adults of females. ATP synthase, citrate synthase, dynamin-related protein 1 and mitochondrial fission factor (Mff) were the highest in sub-adults of females. Peptidylglycine α-amidating monooxygenase were the highest in the aged group, and those of gonadotropin-releasing hormone was the highest in the adult group. LC3II/LC3I, P62, Drp1, Fis, and bax/bcl2 were higher in males than that in females. These results suggest that apoptosis mainly affects growth and development in the HG, whereas autophagy affects aging. The difference of the HG weight and mitochondrial function between sexes is mainly related to the apoptosis.

1. Introduction

The Harderian gland (HG), also known as the glandular lacrimales accessory, is located in the medial orbit and widely exists in vertebrates (Buzzell, 1996; Chieffi et al., 1996). The HG probably plays an important role in the physiological adaption to terrestrial life (Webb et al., 1992). Yet, the results of research on HG are complex and confusing. In many cases, it was indistinguishable from the nictitating membrane gland, until Saki (1981) proposed the criterion for characterizing the mammalian Harderian glands, i.e., tubuloalveolar, ocular glands which secrete lipids by a merocrine mechanism (Sakai, 1981). Even though, there are still species differences in the histology and cellular structure of the HG (Funasaka et al., 2010; Mobini, 2012; Frahmand and Mohammadpour, 2015), whose morphological and biochemical characteristics vary with different developmental stages (Elgayar, 2015; Klećkowska-Nawrot et al., 2015; Dakrory, 2015). The HG exhibits marked sex differences in cell type and porphyrin production (Ramos, and CHávez B, Vilchis F., 2010; Hussein et al., 2015). The porphyrin concentrations of HG are also increased with age in rats (Rodriguez et al., 1992). Studies have shown that the survival strategy of the Harderian gland is based on autophagic processes that are considered a constant renovation system (Tomas-Zapico et al., 2005) and autophagy has potent anti-aging properties (Morishita and Mizushima, 2016). Also the sexual dimorphisms in redox signaling and in autophagy corroborates previous findings and underlines the key role of reactive oxygen species in the regulation of autophagy (Vega-Naredo et al., 2009). So the HG is a perfect model to study autophagic modulation (GARCía-Macia M, Santos-Ledo A, Caballero B, et al., 2019).Yet, the mechanisms underlying the sexual dimorphism and the changes of the HG during aging in mammals remain unclear.

Autophagy and apoptosis are two key processes that control the turnover of cells and cellular components. Many pathways related to

* Corresponding author.
E-mail addresses: catherine_kkk@163.com (X.-T. Kong), qfwz@qfnu.edu.cn (Z. Wang), 1020442922@qq.com (J.-J. Mou), 2990139641@qq.com (C.-S. Li), xuehl@qfnu.edu.cn (H.-L. Xue), wuming@qfnu.edu.cn (M. Wu), cl0624@126.com (L. Chen), xujinhui@qfnu.edu.cn (J.-H. Xu), xulx@qfnu.edu.cn (L.-X. Xu).
[1] Co-first authors.
[2] Contributed to the work equally.

https://doi.org/10.1016/j.cbpb.2020.110547
Received 1 July 2020; Received in revised form 26 October 2020; Accepted 10 December 2020
Available online 17 December 2020
1096-4959/© 2020 Elsevier Inc. All rights reserved.

stress sequentially elicit to autophagy and apoptosis. In general, autophagy inhibits the induction of apoptosis, and apoptosis-associated caspase activation turns off the autophagy process (Marino et al., 2014). Autophagy is a lysosomal degradation process that occurs to eukaryotic cells and is one of the hallmarks of aging. Autophagic activity decreases with age in many species (Uddin et al., 2012; Donati et al., 2001). While current studies have shown that the aging process accompanied by an increase in autophagy levels to remove necrotic organs or substances (Revuelta and Matheu, 2017). Apoptosis is considered to be involved in regulating various processes, including normal cell turnover, proper development and functioning of the immune system, hormone-dependent atrophy and chemical-induced cell death (Elmore, 2007). Importantly, many studies indicate that apoptosis plays a key role in the development of neuroendocrine tissues (Caballero and Coto-Montes, 2012; Cescon et al., 2016).

Autophagic activity on HG was significantly changed during the estrous cycle (Garcia-Macia et al., 2014), melatonin may be one of the main modulators in Syrian hamster (GARCía-Macia M, Santos-Ledo A, Caballero B, et al., 2019). In fact, HG may secrete some hormones such as gonadotropin-releasing hormone (GnRH), thyrotropin-releasing hormone (TRH), and somatostatin (SS) (Mato et al., 1996; Vivien-Roels et al., 1981; Xu et al., 2016).Thus, the detection of GnRH and assessment of TRH secretory function may be helpful in elucidating the secretory function of the HG.

Structure and function of the HG are varying significantly among species. But there is still a lack of reports on the changes of the HG in wildlife with age (Santillo et al., 2020). Striped dwarf hamster (*Cricetulus barabensis*) is a small non-hibernating mammal that is widely distributed in the north temperate zone of Asia (Li et al., 2015; Xu et al., 2017; Xue et al., 2014; Wen et al., 2019). It has some unique physiological characteristics, such as metabolism adapted to cold winter temperatures and daily torpor, etc. That makes it an ideal animal model for the study on wildlife physiological adaptation mechanism. Based on the above contents, the study of hamster's HG in different ages is helpful to further explore the mechanism of HG changes in different states.

Here, we hypothesize that changes in autophagy and apoptotic levels in the HG of hamsters are related to age and sex. We also hypothesized that the level of autophagy and apoptosis in the HG could affect mitochondrial and secretory function. To test these hypotheses, we examined the levels of autophagy and apoptosis in the HG of hamsters during different ages in both sexes. On this basis, changes in mitochondrial division, ATP production, and hormone secretion were further explored to better assess any changes in the HG during growth, development, and aging.

2. Materials and methods

2.1. Ethics statement

All procedures followed the Laboratory Animal Guidelines for the Ethical Review of Animal Welfare (GB/T 35892–2018) and were approved by the Animal Care and Use Committee of Qufu Normal University (Permit Number: dwsc2019010).

2.2. Animals and groups

In March 2019, striped hamsters used in this study were captured by live-trap method using an iron cage in the fields of Mountain, China (N35.78° E117.01°). This area belongs to the temperate continental monsoon, light and temperature changes with the seasons. The main vegetation is wheat, peanuts, and corn.

Captured hamsters were acclimated in the animal feeding room and exposed to natural light until the tissue sampling. Hamsters were housed individually in cages (28 × 18 × 12 cm) at an ambient temperature of 22 ± 2 °C and relative humidity 55% ± 5%. Food (standard rat chow, Pengyue Experimental Animal Breeding Co., Ltd., China) and water were provided ad libitum, wood shavings as bedding.

A total of 60 hamsters were divided into the 3 groups: sub-adult group (S), adult group (A) and aged group (G). There were 20 hamsters in each group, consisting of 10 males and 10 females. All the sub-adult hamsters were born in the March of 2019, with the age of about 1.5 months (10-20 g). The testicular appearance of sub-adult males was not obvious. Sub-adult females had an unopened vagina. Both the adult and the aged hamsters were overwintering, which was mainly distinguished by the body mass in live-trapped, the wear degree of upper molars (Schultz and Martin, 2011) and genital condition (Parkening, 1982). The age of the adult hamsters was between 6 and 12 months (20-30 g), and that of the aged hamsters was between 12 and 18 months (about 30 g). All adults and aged males had visible testes. The vaginal smear method was used to detect the adult and aged female's estrous cycle (Mclean et al., 2012), and hamsters at the anestrus stage were used for tissue sampling. The experiment was carried out in May 2019.

2.3. Sample preparation

The hamsters were sacrificed by CO_2 asphyxiation. The HGs were removed and recorded length and weight. The left HGs was immersed in 4% paraformaldehyde for frozen section embedding. The right HGs was stored in a refrigerator at −80 °C for subsequent western blot experiments (Wang et al., 2020).

2.4. Fluorescence immunohistochemistry analysis

After the fixation in 4% paraformaldehyde for 24 h, dehydration in graded sucrose (10%, 15%, 20%) and washing with 100% acetone, the tissue was embedded in an optimal cutting temperature compound (Sakura, MA, USA). We cut 10-μm thick frozen HGs cross-sections from the mid-belly of each tissue at −20 °C with a cryostat (Leica, Wetzlar, CM1850, Germany). After air drying for 2 h, ten sections from each lobe were randomly selected for follow-up experiments. Sections were cleaned by PBS, then permeation with 0.2% Triton X-100 in 0.1% sodium at 37 °C for 30 min, and the cleared sections were stained in blocking solution [5% bovine serum albumin (BSA)] for 30 min at room temperature and then incubated with rabbit anti-LC3 (1:200, #ab48394, Abcam, Cambridge, UK) or rabbit anti-P62 (1:200, #18420, Proteintech, Wuhan, China) solution at 4 °C overnight. PBS was used as negative control agent instead of primary antibodies. Subsequently, the sections were incubated with goat anti-rabbit Alexa Fluor 488 (1:200, #11034, Thermo Fisher Scientific, Rockford, IL, USA) at 37 °C for 2 h and then with anti-laminin rabbit polyclonal antibody (1:500, #BA1761, Boster, Wuhan, China) and goat anti-rabbit Alexa Fluor 647 (1:200, #21245, Thermo Fisher Scientific). Finally, the sections were counterstained with 4′6'-diamidino-2-phenylindole (DAPI) (1:100, #D1306, Sigma-Aldrich, Saint Quentin Fallavier, France) at 37 °C for 30 min (Fujita et al., 2017). The slides were visualized using a confocal laser scanning microscope (ZEISS, 880NLO, Germany) by illuminating with a krypton/argon laser at wavelengths of 350 nm, 488 nm, 647 nm for excitation, and capturing the fluorescence at the emission wavelength of 461 nm, 526 nm and 665 nm. The number of protein aggregates of LC3 and P62 was counted by selecting an area with dimensions of 100 μm × 100 μm. Quantification analysis was performed with the NIH Image software (Image-pro plus 6.0) (Wang et al., 2020).

2.5. Terminal deoxynucleotidyl transferase biotin-dUTP nick end labeling (TUNEL) staining

DNA fragmentation induced by apoptosis was determined by double-labeled fluorometric TUNEL detection, and evaluation was performed as previously described (Fu et al., 2016). The frozen sections were permeabilized with 0.2% Triton X-100 in 0.1% sodium citrate at 4 °C for 2 min and incubated with an anti-laminin rabbit polyclonal antibody (1500) at 4 °C overnight. After washing with PBS for 30 min, the sections

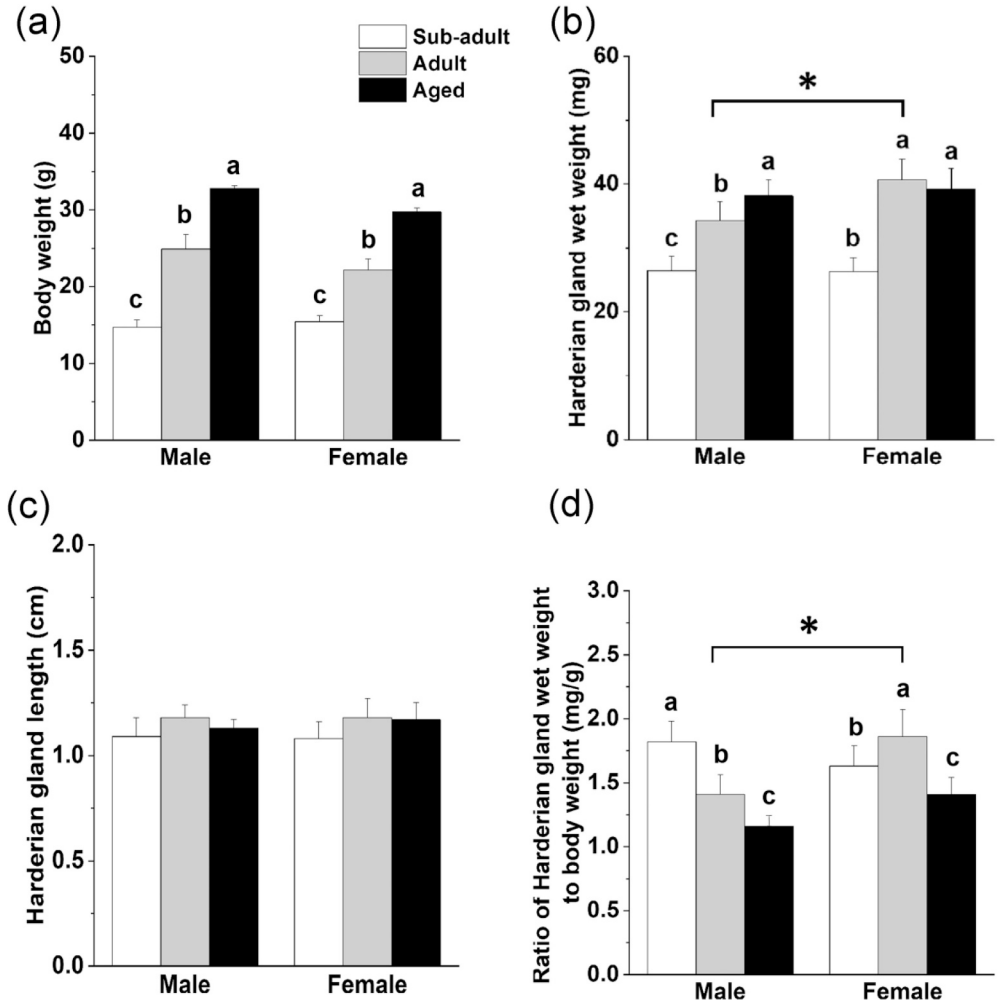

Fig. 1. Effects of age and sex on body weight, Harderian gland wet weight, Harderian gland length and ratio of Harderian gland wet weight to body weight in striped dwarf hamsters (*Cricetulus barabensis*).
Values are represented as the mean ± SD ($n = 10$). Different letters (such as a and b) represent statistically significant differences among three age groups ($P < 0.05$). Same letters (including a and ab) indicate no differences between period groups, and no letters indicate no differences among all six period groups. *, $P < 0.05$ significant difference between male and female.

were incubated with the fluorochrome-conjugated secondary AF647 antibodies at room temperature for 2 h. Subsequently, TUNEL (#MK1023, Boster) reaction mix was added at the recommended 1:9 ratios, and the sections were incubated for 60 min at 37 °C in a humidified chamber in the dark according to the manufacturer's protocol. Finally, the sections were counterstained with DAPI. Imaging was performed using a confocal laser scanning microscope using the same excitation and emission wavelengths as previously described.

2.6. Citrate synthase and caspase3 activity

Samples stored at −80 °C were used to detect citrate synthase and caspase3 activity. Citrate synthase activity was determined by measuring coenzyme A formation at 450 nm with a Citrate Synthase Activity Assay Kit (H-46659, Shanghai Hengyuan Biological Technology Co., Ltd., China) according to the manufacturer's instruction (Song et al., 2018). Caspase3 activity in cell lysates was determined using a Caspase3 Activity Kit (H-46633, Shanghai Hengyuan Biological Technology Co., Ltd., China) following the manufacturer's protocols (Xu et al., 2018).

2.7. Western blotting

Western blot evaluation was performed as previously described (Wang et al., 2019). Protein was extracted from the HGs and solubilized in a sample buffer (100 Mm Tris pH 6.8, 5% 2-β-mercaptoethanol, 5% glycerol, 4% SDS and bromophenol blue), and protein extracts were fractionated by SDS-PAGE using Laemmli gels and transferred to PVDF membranes (0.45 μm pore size) using a Bio-Rad semi-dry transfer apparatus. The blotted membranes were blocked with 1% BSA in Tris-buffered saline (TBS; 150 mM NaCl, 50 mM Tris-HCl, pH 7.5) and incubated with rabbit anti-LC3 (1:1000), rabbit anti-P62 (1:1000), rabbit anti-bax (1:1000, #50599, CST), rabbit anti-bcl2 (1:1000, #3498, proteintech), rabbit anti-Drp1 (1:1000, #12957,proteintech), rabbit anti-Mff (1:1000, #17090,proteintech), rabbit anti-Fis1 (1:1000, #10956, proteintech), rabbit anti-ATP synthase (1:1000, #14676, proteintech), rabbit anti-citrate synthase (1:1000, #16131, proteintech), rabbit anti-PAM (1:1000, #26972, proteintech), rabbit anti-GnRH (1:1000, #DF8553, Affinity Biosciences, OH, USA) and rabbit anti-β-actin (1:5000, #20536, proteintech) in TBS containing 0.1% BSA at 4 °C overnight. The membranes were then incubated with IRDye 800CW goat-anti-rabbit secondary antibodies (1:5000, #31460, Thermo Fisher Scientific) for 90 min at room temperature and visualized with an Odyssey scanner (Bio-rad, California, USA). Quantification analysis of the

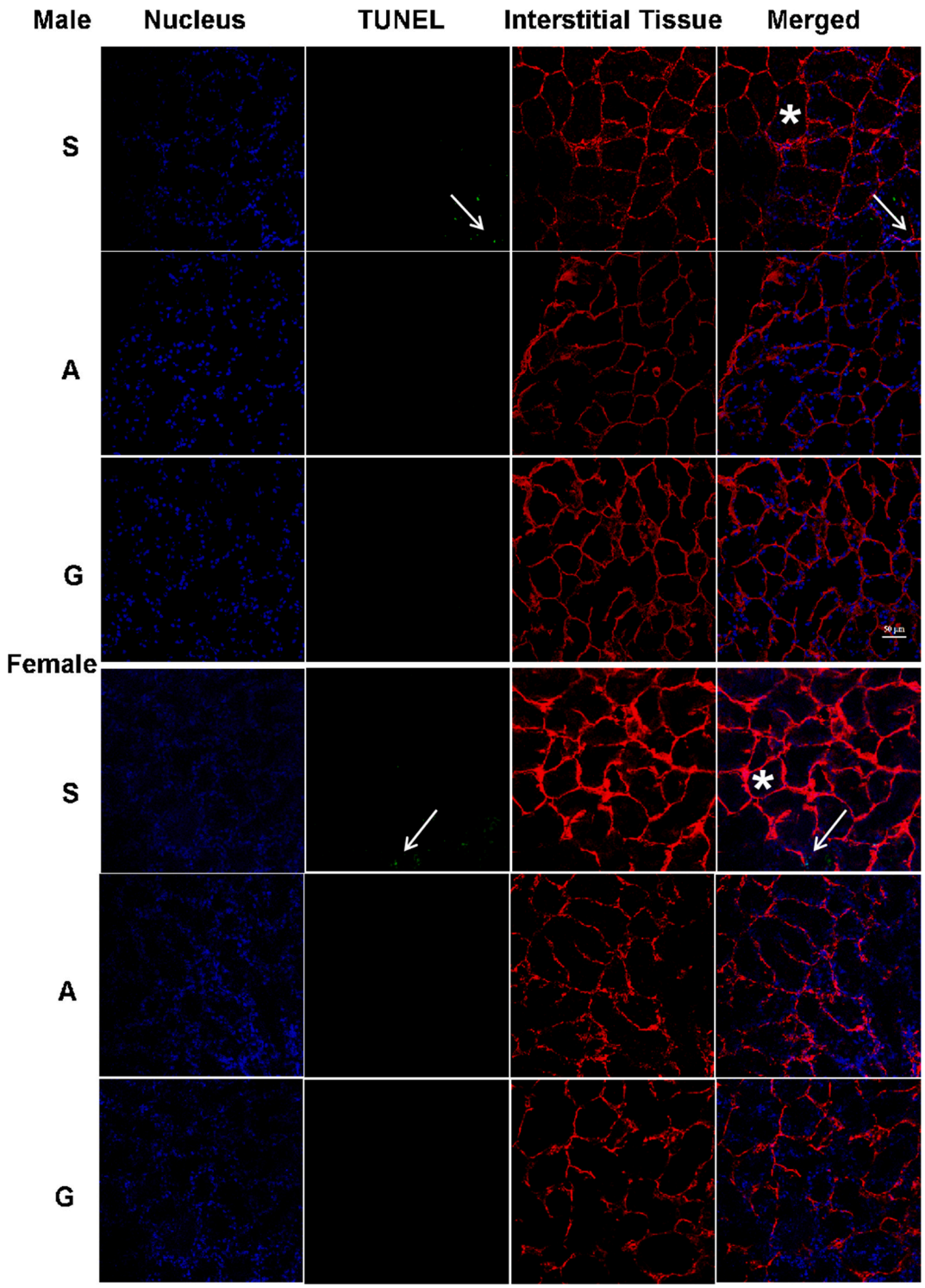

Fig. 2. Fluorescent terminal deoxynucleotidyl transferase biotin-dUTP nick end labeling (TUNEL) stain of HG in striped dwarf hamsters (*Cricetulus barabensis*). Immunofluorescence histochemistry showed cell apoptosis in the HGs of hamsters. Blue represents nucleus by 4′6'-diamidino-2-phenylindole (DAPI), red indicates laminin staining of acinar cavity (*) by Alexa Fluor 647, and green refers to TUNEL (arrow) by FITC. Scale bar = 50 μm. S, sub-adult group; A, adult group; G, aged group.

blots was performed using NIH ImageJ software.

2.8. Statistical analyses

The normality of data and homogeneity of variance were tested by Shapiro-Wilk and Levene, respectively. All data were normal distribution, and the variance was homogeneous. Double factor analysis of variance (two-way ANOVA) was used to compare the in sex and age groups. The differences were considered significant when $P < 0.05$. Data are expressed as means ± standard deviation (Mean ± SD). All statistical analyzes were conducted using SPSS 19.0.

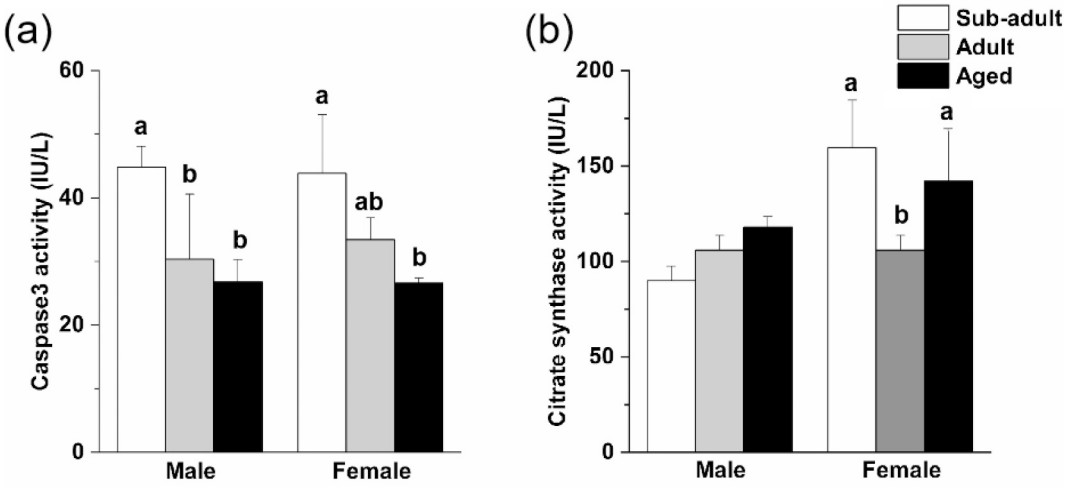

Fig. 3. Activity of caspase3 and CS in the HG of striped dwarf hamsters (*Cricetulus barabensis*).
The activity of caspase3 in three different groups. b) The activity of citrate synthase in three different groups. Values are represented as the mean ± SD. $n = 10$. S, sub-adult group; A, adult group; G, aged group. Different letters (such as a and b) represent statistically significant differences among three age groups ($P < 0.05$). Same letters (including a and ab) indicate no differences between period groups, and no letters indicate no differences among all six period groups. *, $P < 0.05$ significant difference between male and female.

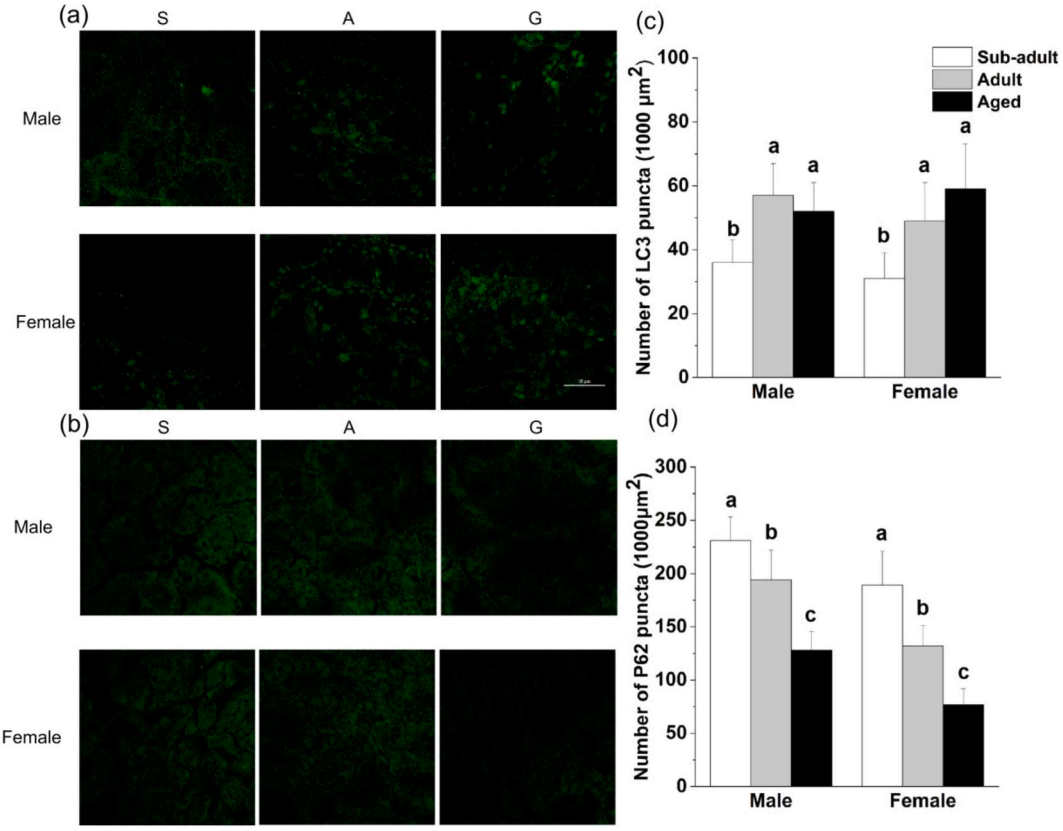

Fig. 4. Quantification of LC3 and P62 puncta in the HG of striped dwarf hamsters (*Cricetulus barabensis*).
(a) Immunofluorescence histochemistry showed LC3 puncta in the HG of hamsters. (d) Immunofluorescence histochemistry showed P62 puncta in the HG of hamsters. (c) Quantification of LC3 puncta. (d) Quantification of P62 puncta. Six Figures were analyzed in each sample; ten samples were analyzed in each group. Values are represented as the mean ± SD. $n = 10$. S, sub-adult group; A, adult group; G, aged group. Different letters (such as a and b) represent statistically significant differences among three age groups ($P < 0.05$). Same letters (including a and ab) indicate no differences between period groups, and no letters indicate no differences among all six period groups. *, $P < 0.05$ significant difference between male and female.

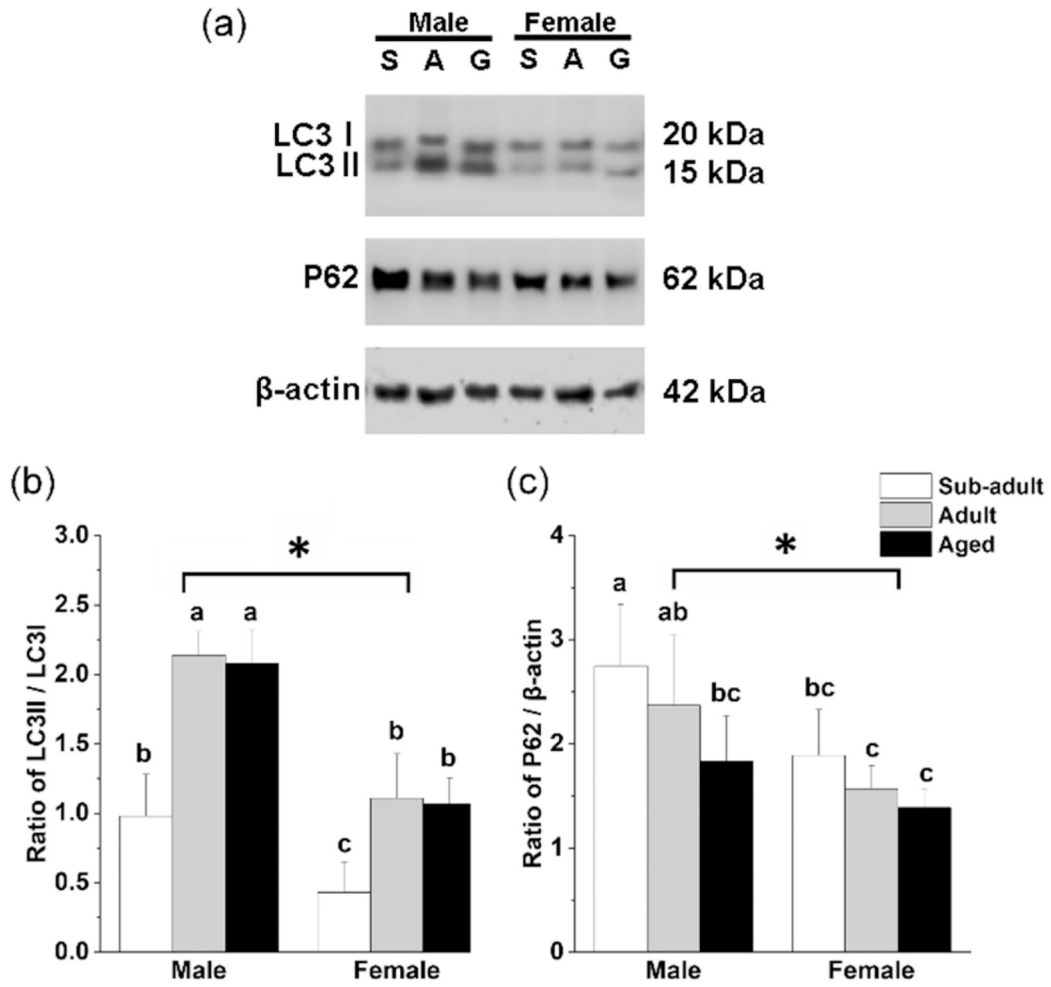

Fig. 5. Changes in the protein expression levels of autophagy related protein in the HG of striped dwarf hamsters (*Cricetulus barabensis*). Representative immunoblots of LC3, P62 and β-actin in three different groups. (b) The ratio of LC3II to LC3I. (c) The ratio of P62 to β-actin. Values are represented as mean ± SD. n = 10. S, sub-adult group; A, adult group; G, aged group. Different letters (such as a and b) represent statistically significant differences among three age groups ($P < 0.05$). Same letters (including a and ab) indicate no differences between period groups, and no letters indicate no differences among all six period groups. *, $P < 0.05$ significant difference between male and female.

3. Results

3.1. Hamsters body weight (BW), Harderian gland wet weight (HGWW), Harderian gland length (HGL) and the ratio of HGWW to body weight (HGWW/BW)

The average body weight of striped dwarf hamsters showed a significant positive correlation with age ($P < 0.05$), whereas there was no significant difference between the sexes. The HGWW in the male hamsters was greater in the aged group ($P < 0.05$), while in the females, no significant difference between the aged and adult groups was observed. The HGL of the hamsters did not significantly differ between ages and sexes. The HGWW/BW in males was S > A > G ($P < 0.05$), while in females, this was A > S > G ($P < 0.05$); and it was higher in females than that in males (Fig. 1).

3.2. DNA fragmentation

TUNEL staining provides direct evidence of apoptosis. Random sections of the HGs showed that DNA fragmentation represented by green fluorescence could hardly be observed in the adult and aged groups of both male and female hamsters. However, in the sub-adult group, green fluorescence was observed in several adjacent cells, and the green fluorescence coincided with the blue fluorescence in the nucleus, indicating increased apoptosis in both male and female sub-adult groups (Fig. 2).

3.3. Changes in CS, and caspase3 activity

Caspase3 activity in the sub-adult group was significantly higher than that in the aged group for both males and females (Fig. 3a), whereas there was no significant difference between the sexes. In male hamsters, the activity of CS increased with age. Whereas in female hamsters, CS were the lowest in adults and the highest in sub-adults. There was no significant difference between the sexes (Fig. 3b).

3.4. The alteration of LC3 and P62 puncta in the HG of hamster of different ages

The number of cytoplasmic LC3 puncta per 1000 μm^2, which is indicative of the conversion of LC3I into LC3II, increased in the adult and aged groups in both male and female hamsters (Fig. 4a, and c).

The number of cytoplasmic P62 puncta per 1000 μm^2 significantly decreased with age in both male and female hamsters and it was higher in males than that in females (Fig. 4b and d).

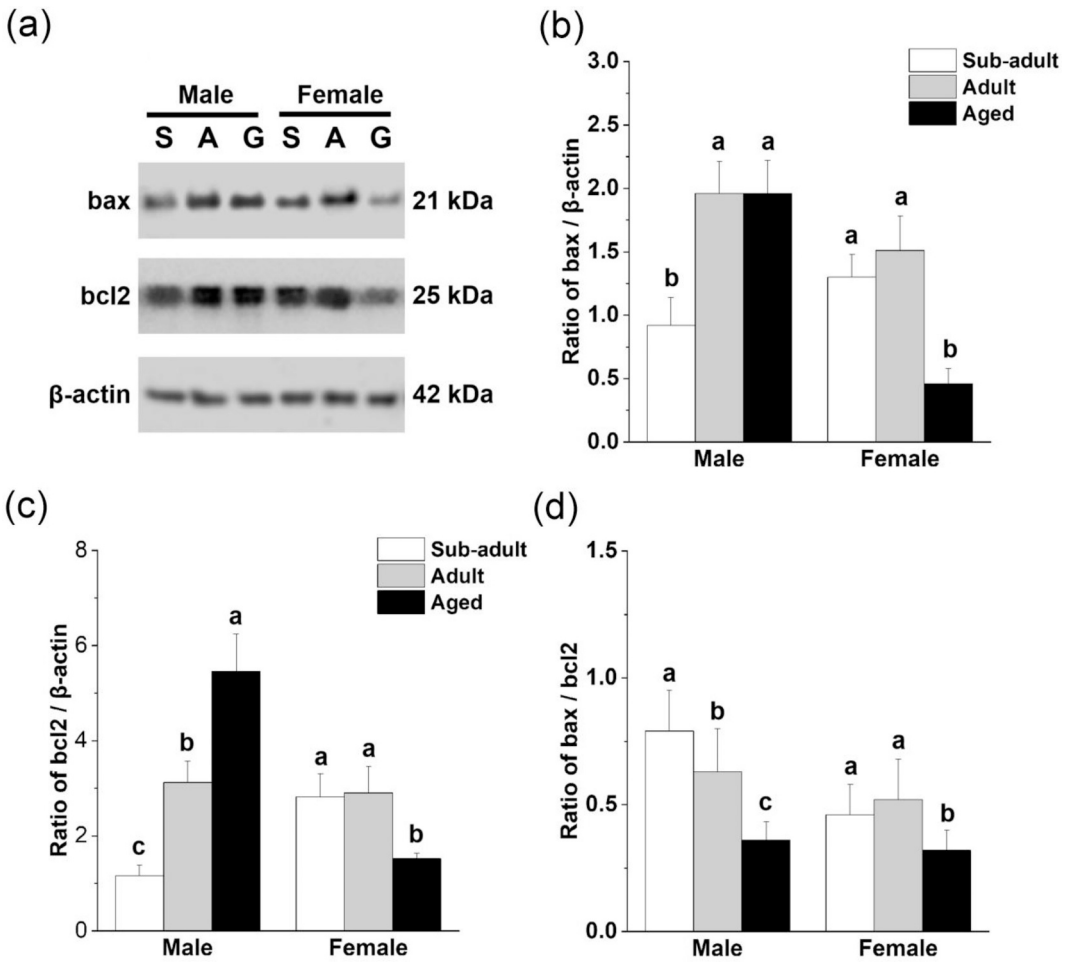

Fig. 6. Changes in the protein expression levels of apoptosis related protein in the HG of striped dwarf hamsters (*Cricetulus barabensis*).
(a) presentative immunoblots of bax, bcl2, and β-actin in three different groups. (b) The ratio of bax to β-actin. (c) The ratio of bcl2 to β-actin. (d) The ratio of bax to bcl2. Values are represented as the mean ± SD. n = 10. S, sub-adult group; A, adult group; G, aged group. Different letters (such as a and b) represent statistically significant differences among three age groups ($P < 0.05$). Same letters (including a and ab) indicate no differences between period groups, and no letters indicate no differences among all six period groups. *, $P < 0.05$ significant difference between male and female.

3.5. Protein expression of autophagy-related factors

LC3I, LC3II, and P62 expression levels were assessed by western blot analysis (Fig. 5a).

LC3II/LC3I protein expression was significantly higher in the adult and aged groups both in males and females, and it was higher in males than that in females ($P < 0.05$) (Fig. 5b).

In contrast to LC3II/LC3I, P62 exhibited a significant decrease in expression with age in both male and female hamsters, and it was higher in males than that in females ($P < 0.05$) (Fig. 5c).

3.6. Protein expression of apoptosis-related factors

The expression levels of bax, and bcl2 were assessed by western blotting (Fig. 6a).

Sex differences in bax and bcl2 protein expression were observed. Bax protein expression in male hamsters showed a significant increase in the adult and aged groups, whereas in female hamsters, it decreased in the aged group compared to the adult and sub-adult groups ($P < 0.05$) (Fig. 6b).

Bcl2 protein expression significantly increased with age in males, while decreased with age in female ($P < 0.05$) (Fig. 6c).

Bax/bcl2 is commonly used to measure the level of mitochondrial apoptosis. It significantly decreased with age in both male and female hamsters ($P < 0.05$) (Fig. 6d).

3.7. Protein expression of mitochondria-related factors

The expression levels of Drp1, Mff, Fis1, ATP synthase and CS were assessed by western blot analysis (Fig. 7a).

The protein expression levels of mitochondrial fission-related genes Drp1, Mff and Fis1 significantly increased in the adult and aged male groups, whereas in females, these significantly decreased in the adult and aged groups, except for Fis1 ($P < 0.05$) (Fig. 7b-d).

The protein expression levels of mitochondrial function-related genes ATP synthase and CS showed significant sex differences such that the protein expression of ATP synthase and CS was higher in the adult and aged male groups but lower in the female adult and aged groups ($P < 0.05$). Except for Mff, the other four indicators were significantly different between sexes ($P < 0.05$) (Fig. 7e and f).

3.8. Relative protein expression of hormone secretion-related factors

The expression levels of Peptidylglycine-α-amidating monooxygenase (PAM) and GnRH were assessed by western blot analysis (Fig. 8a).

PAM protein expression in the aged male and female groups was significantly higher, and it was higher in males than that in females ($P < 0.05$) (Fig. 8b). GnRH protein expression was significantly higher in the adult groups in both the male and female hamsters ($P < 0.05$) (Fig. 8c).

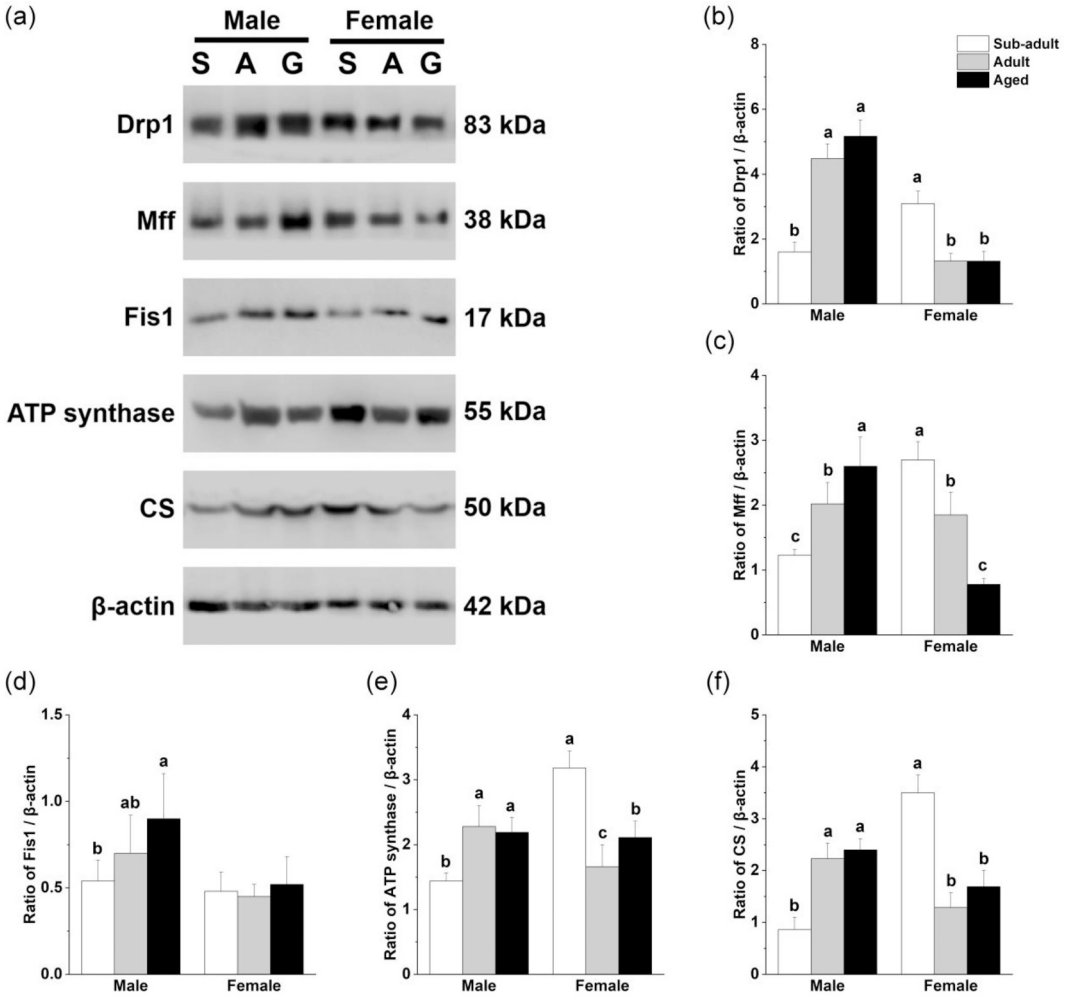

Fig. 7. Changes in the protein levels of mitochondrial related protein in the HG of striped dwarf hamsters (*Cricetulus barabensis*). Representative immunoblots of Drp1, Mff, Fis1, ATP synthase, CS and β-actin in three different groups. (b) The ratio of Drp1 to β-actin. (c) The ratio of Mff to β-actin. (d) The ratio of Fis1 to β-actin. (e) The ratio of ATP synthase to β-actin. (f) The ratio of CS to β-actin. Values are represented as the mean ± SD. n = 10. S, sub-adult group; A, adult group; G, aged group. Different letters (such as a and b) represent statistically significant differences among three age groups ($P < 0.05$). Same letters (including a and ab) indicate no differences between period groups, and no letters indicate no differences among all six period groups. *, $P < 0.05$ significant difference between male and female.

4. Discussion

Our results showed that independent of sex, the level of autophagy in adult and aged hamsters was significantly higher than that in sub-adult hamsters in HGs, whereas the level of apoptosis in sub-adult hamsters was significantly higher than that in adult and aged hamsters. Unexpectedly, ATP synthase and CS protein expression in mitochondria were lowest in sub-adult males but highest in sub-adult females. In addition, the protein expression of Drp1, Fis1 and bax/bcl2 were higher in males than that in females.

The body weight of the hamsters and wet weight of the HG increased with age, but the ratio of HG weight to body weight showed a decreasing trend with age. This indicates that the growth and development of HG were in direct proportion to the growth and development of animals, but the growth rate of HG may be lower than that of the whole body of animals. This result is consistent with the report that the growth of HG was always less than the body as a whole after 15 days of life. Besides, there was no significant difference in the length of the HG at different ages and between sexes. Studies have shown that the size of the eyeball and the length of the eye axis in mammals such as humans and rabbits do not significantly change after sub-adult (Bekerman et al., 2014; Liu et al., 2000). Because the HG is semi-encapsulated in orbit, the maintenance of the length of HG may be related to the stability of the size of the eyeball. In addition, the ratio of HG weight to body weight was significantly higher in females than in males, which is mainly due to the lower HG weight in males (Vianna et al., 1975).

In this study, the ratio of LC3II to LC3I in HG was significantly higher in the adult and aged groups than in the sub-adult group, while the protein expression of P62 was lowest in the aged group, suggesting that the autophagy level in the HG increases with age both in male and female hamsters. This result is different from some studies, which have shown that the level of autophagy in rat liver, mouse skeletal muscle and human skin decreases with age (Uddin et al., 2012; Donati et al., 2001; Chang et al., 2017; Simonsen et al., 2008; Jiao and Demontis, 2017), but this result is similar to the studies of the brain in rats and mice, which showed that autophagy levels in older individuals were significantly higher than younger individuals (Gong et al., 2011; Soontornniyomkij et al., 2012). These conflicting results suggest that the changes of autophagy level with aging may be organ specificity. It is well known that many age-related diseases, such as Sarcopenia and cataract, arise from defective protein degradation and consequent accumulation of misfolded proteins and dysfunctional organelles and that autophagy can ameliorate proteostasis in such conditions (Douglas, Peter, M., et al., 2010). Autophagy inhibition induces hypotrophy, porphyria and tissue

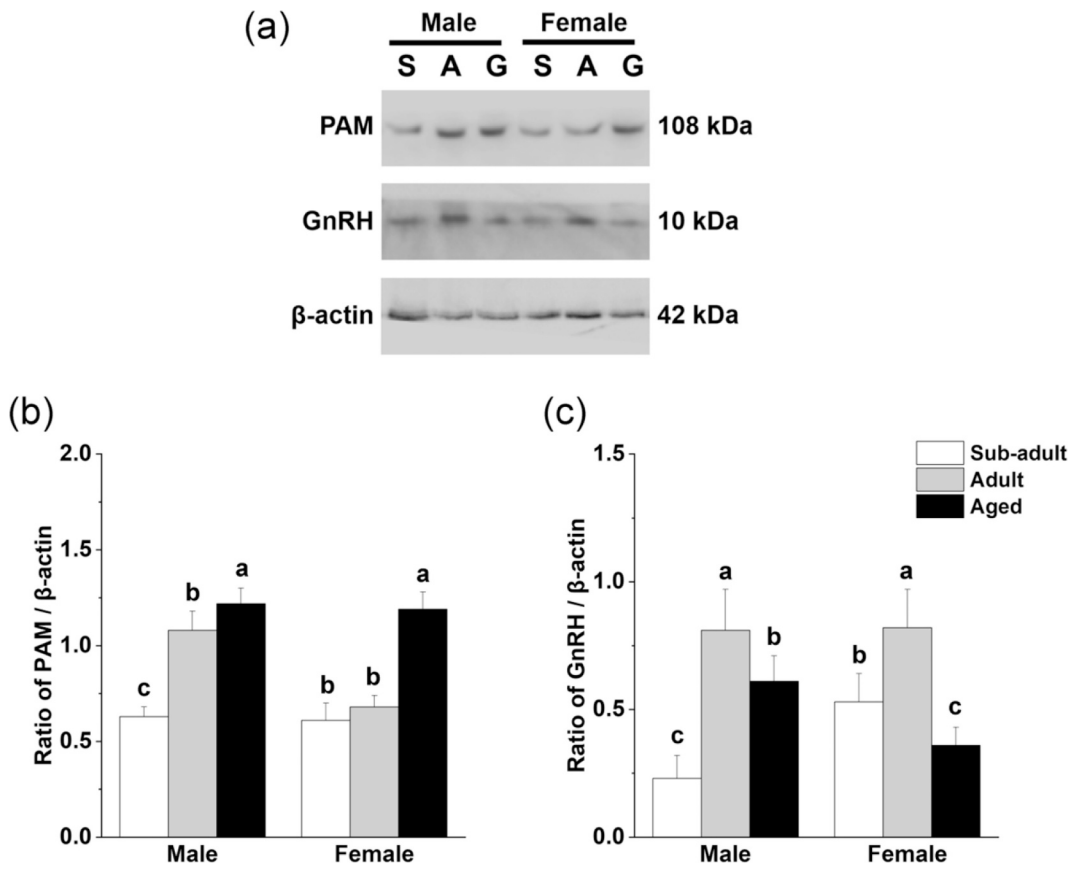

Fig. 8. Changes in the protein expression levels of hormone related protein in the HG of striped dwarf hamsters (*Cricetulus barabensis*).
Representative immunoblots of PAM, GnRH and β-actin in three different groups. (b) The ratio of PAM to β-actin. (C) The ratio of GnRH to β-actin. Values are represented as mean ± SD. n = 10. S, sub-adult group; A, adult group; G, aged group. Different letters (such as a and b) represent statistically significant differences among three age groups ($P < 0.05$). Same letters (including a and ab) indicate no differences between period groups, and no letters indicate no differences among all six period groups. *, $P < 0.05$ significant difference between male and female.

degeneration in the HG (Koenig et al., 2015). We speculate that wild striped dwarf hamsters have improved the autophagy level may help to remove the accumulated toxic substances and keep the normal HG function during the development process, so as to prevent the degeneration of HG. P62 is shown involved in lipophagy and mitophagy (Svenning and Johansen, 2013; Bjorkoy et al., 2005; Sandoval et al., 2008), which may be responsible for the decline in P62 expression. In addition, the protein expression of LC3II/LC3I and P62 were higher in males than that in females. Due to the two proteins represent the up and down-regulation of autophagy, there may be no significant difference in autophagy levels between sexes.

Another important finding of this study was that DNA fragmentation increased in both male and female sub-adult hamsters since the DNA fragmentation is one of the most important indicators of increased apoptotic levels (Smith et al., 2000), this result suggests an increase in apoptotic levels in sub-adults. Bax/bcl2 is often used as a measure of mitochondrial apoptosis (Antonsson et al., 1997; Korsmeyer et al., 1993). Compared with adult hamsters, the protein expression levels of bax/bcl2 in male sub-adults significantly increased, implying the up-regulation of apoptosis, which indicated the activation of the mitochondrial apoptotic pathway, which may be one of the mechanisms underlying the increase in apoptotic levels in male sub-adults. Caspase3 is the effector of apoptosis (Manickam et al., 2017). The activity of caspase3 showed a similar trend, in the sub-adult group was significantly higher than that in the aged group for both males and females. The above results indicate that the apoptosis level of the sub-adults is the highest and the old body is the lowest. This is similar to the results in the thyroid gland of the golden hamster, which showed that apoptotic levels are highest in the sub-adult developmental stage (Chen et al., 2000). We speculate that the increase in apoptotic levels in the HG of sub-adult hamsters may be related to changes in its structure and function during adolescence. In addition, the protein expression of bax/bcl2 in males was significantly higher than that in females, suggesting that the apoptosis level of HG may higher in males, which may be a major factor for the HG weight in males to be lower than that in females.

We also found that the protein expression levels of ATP synthase and CS decreased in male sub-adult hamsters but increased in female sub-adult hamsters compared with that in adult and aged hamsters, indicating significant gender differences. CS is a limiting enzyme of the tricarboxylic acid cycle (Remington, 1992; Wiegand and Remington, 1986), and the ATP synthase is a rate-limiting enzyme in ATP synthesis pathway (Kramarova et al., 2008). In male hamsters, the protein expression levels of ATP synthase and CS increased with age, whereas in female hamsters, those of ATP synthase and CS were the lowest in adults and the highest in sub-adults, and the activity of CS showed a similar trend, suggesting that the function of the mitochondria varies with age and sex. An interesting change, however, is that mitochondrial function was lowest in sub-adult males and highest in females. We believe that this may be related to the changes in cell proliferation, differentiation, and tissue function, which are required for puberty growth and development. These processes are inseparable from the involvement of mitochondrial apoptosis and fission.

Drp1 and Mff are the most important factors that promote mitochondrial fission, whereas Fis1 inhibits Drp1 activity (Kraus and Ryan, 2017; Tilokani et al., 2018). In the HGs of male hamsters, bax/bcl2 protein expression levels increase while Drp1 and Mff protein expression

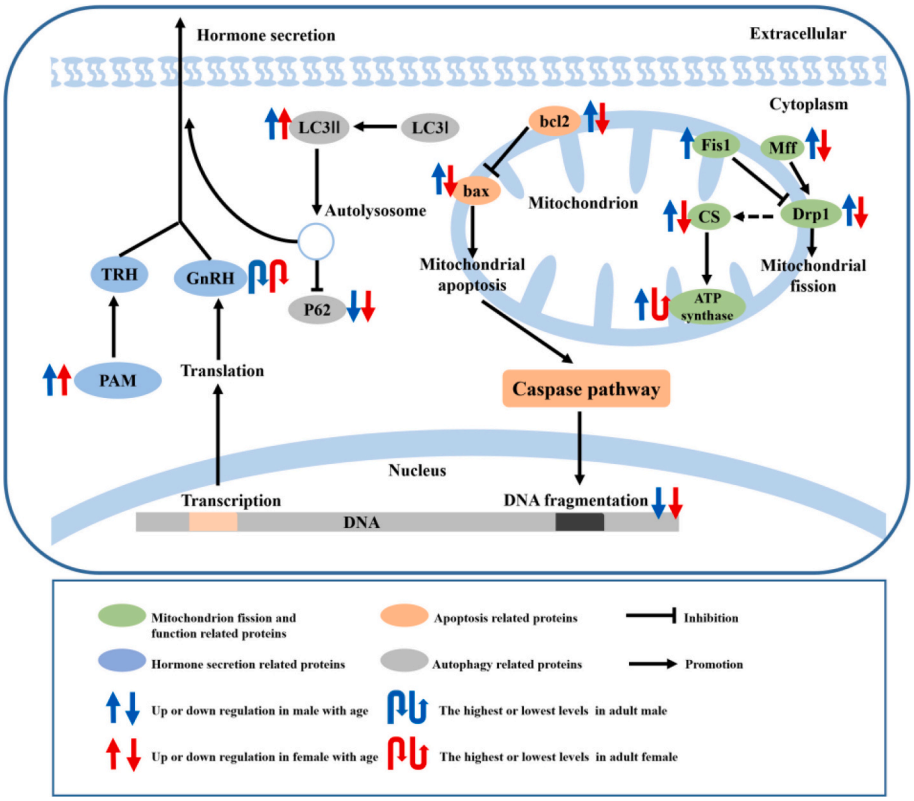

Fig. 9. Graphical summary of the study.
LC3, microtubule-associated protein 1 light chain; P62, sequestosome 1; Fis1, fission 1; Mff, mitochondrialfission factor; Drp1, adynamin-related protein 1; ATP synthase, adenosine triphosphate synthase; CS, citrate synthase; GnRH, gonadotropin-releasing hormone; PAM, Peptidylglycine-α-amidating monooxygenase.

levels decrease in sub-adult group, indicating that the level of mitochondrial apoptosis increased and the level of mitochondrion fission decreased, which may be one of the main reasons for the decreased mitochondrial function. In the HGs of female hamsters, bax/bcl2 protein expression levels maintain while Drp1 and Mff protein expression levels increase in sub-adult group, indicating that the level of mitochondrial apoptosis maintained and the level of mitochondrion fission increased, which may be one of the main reasons for the enhancement of mitochondrial function. In general, the significant changes of mitochondrion fission level between sexes may be one of the main reasons for the significant differences of mitochondrion function in the HGs of the sub-adults. In addition, the protein expression of ATP synthesis in males was lower than that in females. The protein expression of Drp1 and Fis1 was higher in males than that in females, suggesting that the mitochondrion fission level might not be different between males and females. Therefore, the apoptosis level in males is higher than that in females, which may be one of the main reasons for the difference of ATP synthesis protein expression between sexes.

In addition, PAM protein expression was the highest in the aged group, whereas GnRH protein expression was the highest in the HG of adult male and female hamsters. GnRH is a neurohormone that is mainly secreted by the hypothalamus and plays an important role in the regulation of vertebrate reproduction (Kaprara and Huhtaniemi, 2018). In this study, GnRH protein expression was highest in adult HGs, which was consistent with animal reproduction peak in adults. Studies on male rats showed that GnRH protein expression levels in the hypothalamus of elderly individuals were lower than adult animals (Gruenewald and Matsumoto, 1991; Jarjour et al., 1986). The results of this study were similar to those of rats. PAM is the final rate-limiting enzyme formed by TRH in cells, which can amide the precursor to form TRH (Milgram et al., 1996). Studies have shown that TRH secretion in the brain of aged (22–24 months) rats was significantly higher than that of young (3–5 months) rats (Donda et al., 1989). Our results show that autophagy levels are high in the HG of adult and aged groups. In view of the fact that autophagy itself is a form of hormone secretion (Koenig et al., 2015), we speculate that the high levels of expression of GnRH and PAM may be related to the enhancement of autophagic function.

5. Conclusions

In summary, we present a finding involving autophagy, apoptosis, mitochondrial changes, and synthesis mechanisms of the HG in hamsters at different ages and sexes using multiple techniques (Fig. 9). We demonstrate that the apoptotic level of the HG is highest in sub-adults, which may be related to changes in its structure and function during adolescence. Autophagy levels are highest in the aged individuals of both sexes. Mitochondrial function in HGs of sub-adults significantly changes between males and females, which may be related to mitochondrion fission level. The protein expression of GnRH and PAM is the highest in adult and aged groups respectively, which may be related to the change of reproductive age and autophagy level of hamsters. The protein expression of ATP synthesis and the HG weight between sexes were lower in males, which may be related to the higher apoptosis level in HG of male hamsters. In general, apoptosis mainly affects growth and development in the HG, whereas autophagy affects aging, which influences the endocrine function of the HG in adult and sub-adult; the difference of the HG weight and mitochondrial function between sexes is mainly related to the apoptosis level.

Declaration of Competing Interest

None.

Acknowledgments

We thank LetPub (www.letpub.com) for its linguistic assistance during the preparation of this manuscript. This work was supported by grants (31670385, 31770455, and 31570377) from the National Natural Science Foundation of China (https://isisn.nsfc.gov.cn) to L.-X.X., J.-H. X. and H.-L.X, respectively. The funders had no role in study design, data collection and analysis, decision to publish, or preparation of the manuscript.None of the authors has a conflict of interest.

Appendix A. Supplementary data

Supplementary data to this article can be found online at https://doi.org/10.1016/j.cbpb.2020.110547.

References

Antonsson, B., Conti, F., Ciavatta, A., et al., 1997. Inhibition of Bax channel-forming activity by Bcl-2 [J]. Science 277 (5324), 370–372.
Bekerman, I., Gottlieb, P., Vaiman, M., 2014. Variations in eyeball diameters of the healthy adults [J]. J. Ophthalmol. 5.
Bjorkoy, G., Lamark, T., Brech, A., et al., 2005. p62/SQSTM1 forms protein aggregates degraded by autophagy and has a protective effect on huntingtin-induced cell death [J]. J. Cell Biol. 171 (4), 603–614.
Buzzell, G.R., 1996. The Harderian gland: perspectives [J]. Microsc. Res. Tech. 34 (1), 2–5.
Caballero, B., Coto-Montes, A., 2012. An insight into the role of autophagy in cell responses in the aging and neurodegenerative brain [J]. Histol. Histopathol. 27 (3), 263–275.
Cescon, M., Chen, P., Castagnaro, S., et al., 2016. Lack of collagen VI promotes neurodegeneration by impairing autophagy and inducing apoptosis during aging [J]. Aging-US 8 (5), 1083–1101.
Chang, J.T., Kumsta, C., Hellman, A.B., et al., 2017. Spatiotemporal regulation of autophagy during *Caenorhabditis elegans* aging [J]. Elife 6 (23).
Chen, H., Hayakawa, D., Emura, S., et al., 2000. Occurrence of the parathyroid cyst in golden hamsters [J]. Annals of anatomy =. Anatomischer Anzeiger 182 (6), 493–498.
Chieffi, G., Baccari, G.C., Di Matteo, L., et al., 1996. Cell biology of the harderian gland [J]. Int. Rev. Cytol. 168, 1–80.
Dakrory, A.I., 2015. Early embryonic development of the Harderian gland of the common quail (*Coturnix coturnix*) [J]. Bulgarian J. Veterinary Med. 18 (4), 304–312.
Donati, A., Cavallini, G., Paradiso, C., et al., 2001. Age-related changes in the autophagic proteolysis of rat isolated liver cells: effects of antiaging dietary restrictions [J]. J. Gerontol. A Biol. Sci. Med. Sci. 56 (9), B375–B383.
Donda, A., Reymond, M.J., Lemarchand-Beraud, T., 1989. Influence of age on the control of thyrotropin secretion by thyrotropin-releasing hormone in the male rat [J]. Neuroendocrinology 49 (4), 389–394.
Douglas, Peter, M., et al., 2010. Protein homeostasis and aging in neurodegeneration [J]. J. Cell Biol. 190 (5), 719–729.
Elgayar, S., 2015. Morphology of female Guinea pig Harderian gland during postnatal development - secretory endpieces [J]. Eur. J. Anat. 19 (1), 15–26.
Elmore, S., 2007. Apoptosis: a review of programmed cell death [J]. Toxicol. Pathol. 35 (4), 495–516.
Frahmand, S., Mohammadpour, A.A., 2015. Harderian gland in Canadian ostrich (*Struthio camelus*): A morphological and histochemical study [J]. Anat. Histol. Embryol. 44 (3), 178–185.
Fu, W.W., Hu, H.X., Dang, K., et al., 2016. Remarkable preservation of Ca2+ homeostasis and inhibition of apoptosis contribute to anti-muscle atrophy effect in hibernating Daurian ground squirrels [J]. Sci. Rep. 6 (13).
Fujita, N., Huang, W., T-H, L.I.N., et al., 2017. Genetic screen in Drosophila muscle identifies autophagy-mediated T-tubule remodeling and a Rab2 role in autophagy [J]. Elife 6.
Funasaka, N., Yoshioka, M., Fujise, Y., 2010. Features of the ocular Harderian gland in three Balaenopterid species based on anatomical, histological and histochemical observations [J]. Mamm Study 35 (1), 9–15.
GARCía-Macia M, Santos-Ledo A, Caballero B, et al., 2019. Selective autophagy, lipophagy and mitophagy, in the Harderian gland along the oestrous cycle: a potential retrieval effect of melatonin [J]. Sci. Rep. 9 (1), 18597.
Garcia-Macia, M., Rubio-Gonzalez, A., De Luxan-Delgado, B., et al., 2014. Autophagic and proteolytic processes in the Harderian gland are modulated during the estrous cycle [J]. Histochem. Cell Biol. 141 (5), 519–529.
Gong, Y., He Y, Gu Y, et al., 2011. Effects of aging on autophagy after experimental intracerebral hemorrhage [J]. Acta Neurochir. Suppl. 111 (113–7).
Gruenewald, D.A., Matsumoto, A.M., 1991. Age-related decreases in serum gonadotropin levels and gonadotropin-releasing hormone gene expression in the medial preoptic area of the male rat are dependent upon testicular feedback [J]. Endocrinology 129 (5), 2442–2450.
Hussein, O.A., Elgamal, D.A., Elgayar, S.A., 2015. Structure of the secretory cells of male and female adult Guinea pigs Harderian gland [J]. Tissue Cell 47 (3), 323–335.
Jarjour, L.T., Handelsman, D.J., Swerdloff, R.S., 1986. Effects of aging on the in vitro release of gonadotropin-releasing hormone [J]. Endocrinology 119 (3), 1113–1117.
Jiao, J., Demontis, F., 2017. Skeletal muscle autophagy and its role in sarcopenia and organismal aging [J]. Curr. Opin. Pharmacol. 34 (1–6).
Kaprara, A., Huhtaniemi, I.T., 2018. The hypothalamus-pituitary-gonad axis: Tales of mice and men [J]. Metab. Clin. Exp. 86 (3–17).
Klećkowska-Nawrot, J., GOŹdziewska-Harłajczuk, K., Barszcz, K., et al., 2015. Morphological studies on the harderian gland in the ostrich (Struthio camelus domesticus) on the embryonic and post-natal period [J]. Anat. Histol. Embryol. 44 (2), 146–156.
Koenig, U., Fobker, M., Lengauer, B., et al., 2015. Autophagy facilitates secretion and protects against degeneration of the Harderian gland [J]. Autophagy 11 (2), 298–313.
Korsmeyer, S.J., Shutter, J.R., Veis, D.J., et al., 1993. Bcl-2/Bax: a rheostat that regulates an anti-oxidant pathway and cell death [J]. Semin. Cancer Biol. 4 (6), 327–332.
Kramarova, T.V., Shabalina, I.G., Andersson, U., et al., 2008. Mitochondrial ATP synthase levels in brown adipose tissue are governed by the c-Fo subunit P1 isoform [J]. FASEB J. 22 (1), 55–63.
Kraus, F., Ryan, M.T., 2017. The constriction and scission machineries involved in mitochondrial fission [J]. J. Cell Sci. 130 (18), 2953–2960.
Li, S.N., Xue, H.L., Zhang, Q., et al., 2015. photoperiod regulates the differential expression of KiSS-1 and GPR54 in various tissues and sexes of striped hamster [J]. Genet. Mol. Res. 14 (4), 13894–13905.
Liu, J.H., Farid, H., Rapaport, D.H., 2000. Sympathetic nervous system plays a role in postnatal eyeball enlargement in the rabbit [J]. Invest. Ophthalmol. Vis. Sci. 41 (9), 2684–2688.
Manickam, P., Kaushik, A., Karunakaran, C., et al., 2017. Recent advances in cytochrome c biosensing technologies [J]. Biosens. Bioelectron. 87 (654–68).
Marino, G., Niso-Santano, M., Baehrecke, E.H., et al., 2014. Self-consumption: the interplay of autophagy and apoptosis [J]. Nat. Rev. Mol. Cell Biol. 15 (2), 81–94.
Mato, M.E., Puig-Domingo, M., Fornas, O., et al., 1996. Expression of the somatostatin gene and receptors in the rat harderian gland [J]. Microsc. Res. Tech. 34 (2), 118–122.
Mclean, A.C., Valenzuela, N., Fai, S., et al., 2012. Performing Vaginal Lavage, Crystal Violet Staining, and Vaginal Cytological Evaluation for Mouse Estrous Cycle Staging Identification [J]. Jove-J. Visual. Exp. 67.
Milgram, S.L., Mains, R.E., Eipper, B.A., 1996. Identification of routing determinants in the cytosolic domain of a secretory granule-associated integral membrane protein [J]. J. Biol. Chem. 271 (29), 17526–17535.
Mobini, B., 2012. Histological and histochemical studies on the Harderian gland in native chickens [J]. Vet. Med. 57 (8), 404–409.
Morishita, H., Mizushima, N., 2016. Autophagy and ageing [J]. Nihon rinsho Japanese J. Clin. Med. 74 (9), 1461–1466.
Parkening, T.A., 1982. Reproductive senescence in the Chinese hamster (Cricetulus griseus) [J]. J. Gerontol. 37 (3), 283–287.
Ramos, L., CHávez B, Vilchis F., 2010. Cloning and differential expression of steroid 5 alpha-reductase type 1 (Srd5a1) and type 2 (Srd5a2) from the Harderian glands of hamsters [J]. Gen. Comp. Endocrinol. 166 (2), 388–395.
Remington, S.J., 1992. Structure and mechanism of citrate synthase [J]. Curr. Top. Cell. Regul. 33 (209–29).
Revuelta, M., Matheu, A., 2017. Autophagy in stem cell aging [J]. Aging Cell 16 (5), 912–915.
Rodriguez, C., Menendez-Pelaez, A., Howes, K.A., et al., 1992. Age and food restriction alter the porphyrin concentration and mRNA levels for 5-aminolevulinate synthase in rat Harderian gland [J]. Life Sci. 51 (24), 1891–1897.
Sakai, T., 1981. The mammalian Harderian gland: morphology, biochemistry, function and phylogeny [J]. Archivum Histologicum Japonicum = Nihon soshikigaku kiroku 44 (4), 299–333.
Sandoval, H., Thiagarajan, P., Dasgupta, S.K., et al., 2008. Essential role for nix in autophagic maturation of erythroid cells [J]. Nature 454 (7201), 232–U66.
Santillo, A., Baccari, G.C., Minucci, S., et al., 2020. The Harderian gland: Endocrine function and hormonal control [J]. Gen. Comp. Endocrinol. 297.
Schultz, J.A., Martin, T., 2011. Wear pattern and functional morphology of dryolestoid molars (Mammalia, Cladotheria) [J]. Palaontol Z 85 (3), 269–285.
Simonsen, A., Cumming, R.C., Brech, A., et al., 2008. Promoting basal levels of autophagy in the nervous system enhances longevity and oxidant resistance in adult Drosophila [J]. Autophagy 4 (2), 176–184.
Smith, H.K., Maxwell, L., Martyn, J.A., et al., 2000. Nuclear DNA fragmentation and morphological alterations in adult rabbit skeletal muscle after short-term immobilization [J]. Cell Tissue Res. 302 (2), 235–241.
Song, M., F-F, C.H.E.N., Y-H, L.I., et al., 2018. Trimetazidine restores the positive adaptation to exercise training by mitigating statin-induced skeletal muscle injury [J]. J. Cachexia. Sarcopenia Muscle 9 (1), 106–118.
Soontornniyomkij, V., Risbrough, V.B., Young, J.W., et al., 2012. Increased hippocampal accumulation of autophagosomes predicts short-term recognition memory impairment in aged mice [J]. Age 34 (2), 305–316.
Svenning, S., Johansen, T., 2013. Selective autophagy [M]//LANE J D. Autophagy 79–92.
Tilokani, L., Nagashima, S., Paupe, V., et al., 2018. Mitochondrial dynamics: overview of molecular mechanisms [J]. Essays Biochem. 62 (3), 341–360.
Tomas-Zapico, C., Caballero, B., Sierra, V., et al., 2005. Survival mechanisms in a physiological oxidative stress model [J]. FASEB J. 19 (14), 2066–2068.
Uddin, M.N., Nishio, N., Ito, S., et al., 2012. Autophagic activity in thymus and liver during aging [J]. Age 34 (1), 75–85.
Vega-Naredo, I., Caballero, B., Sierra, V., et al., 2009. Sexual dimorphism of autophagy in Syrian hamster Harderian gland culminates in a holocrine secretion in female glands [J]. Autophagy 5 (7), 1004–1017.

Vianna, G.F., Cruz, A.R., Azoubel, R., 1975. Allometric study of the lachrymal and Harderian glands of the rat during postnatal life [J]. Acta Anat. 92 (2), 161–170.
Vivien-Roels, B., Pevet, P., Dubois, M.P., et al., 1981. Immunohistochemical evidence for the presence of melatonin in the pineal gland, the retina and the Harderian gland [J]. Cell Tissue Res. 217 (1), 105–115.
Wang, Z., Jiang, S.F., Cao, J., et al., 2019. Novel findings on ultrastructural protection of skeletal muscle fibers during hibernation of Daurian ground squirrels: mitochondria, nuclei, cytoskeleton, glycogen [J]. J. Cell. Physiol. 234 (8), 13318–13331.
Wang, Z., J-H, X.U., J-J, M.O.U., et al., 2020. Photoperiod Affects Harderian Gland Morphology and Secretion in Female *Cricetulus barabensis*: Autophagy, Apoptosis, and Mitochondria [J]. Front. Physiol. 11(408).
Webb, S.M., Puig-Domingo, M., Viader, M., et al., 1992. Harderian Gland Peptides [M].
Wen, J., Q-G, Q.I.A.O., Z-J, Z.H.A.O., et al., 2019. Effects of thyroid hormones and cold acclimation on the energy metabolism of the striped hamster (Cricetulus barabensis) [J]. J. Compar. Physiol. B-Biochem. Syst. Environ. Physiol. 189 (1), 153–165.
Wiegand, G., Remington, S.J., 1986. Citrate synthase: structure, control, and mechanism [J]. Annu. Rev. Biophys. Biophys. Chem. 15 (97–117).
Xu, Y., Yao, Y., Jiang, X., et al., 2018. SP1-induced upregulation of lncRNA SPRY4-IT1 exerts oncogenic properties by scaffolding EZH2/LSD1/DNMT1 and sponging miR-101-3p in cholangiocarcinoma [J]. J. Exp. Clin. Cancer Res. 37.
Xu, J., Geng, X., Chen, L., et al., 2016. Differential expression of somatostatin in the Harderian glands of different gender/age Cricetulus barabensis [J]. Acta Theriologica Sinica 36 (4), 429–437.
Xu, L.X., Xue, H.L., Li, S.N., et al., 2017. Seasonal differential expression of KiSS-1/GPR54 in the striped hamsters (Cricetulus barabensis) among different tissues [J]. Integr Zool 12 (3), 260–268.
Xue, H.L., Xu, J.H., Chen, L., et al., 2014. Genetic variation of the striped hamster (*Cricetulus barabensis*) and the impact of population density and environmental factors [J]. Zool. Stud. 53 (8).